Title: Regulation of human feto-placental endothelial barrier integrity by vascular endothelial growth factors: competitive interplay between VEGF-A_{165}a, VEGF-A_{165}b, PIGF and VE-cadherin.

Vincent Pang[1,2], David O Bates[1*], Lopa Leach[2*]

[1]Cancer Biology, Division of Cancer and Stem Cells, School of Medicine, and [2]School of Life Sciences, University of Nottingham, Queen's Medical Centre, Nottingham NG2 7UH

*Authors for correspondence

David.Bates@nottingham.ac.uk, Lopa.Leach@nottingham.ac.uk

Keywords. VEGF, permeability, placenta, VE-cadherin

Running title: VEGF isoforms in placental permeability

Abbreviations:

Adherens junction (AJ), Vascular endothelial growth factor (VEGF), Placental growth factor (PIGF), Vascular endothelial growth factor receptor-1 (VEGFR1), Vascular endothelial growth factor receptor-2 (VEGFR2), Vascular endothelial-cadherin (VE-cadherin), Human umbilical vascular endothelial cell (HUVEC), Fms-like tyrosine kinase (Flt-1), Soluble fms-like tyrosine kinase (sFlt-1), Fluorescein isothiocyanate-conjugated bovine serum albumin (FITC-BSA), Tetramethylrhodamine isothiocyanate (TRITC), Signal transducer and activator of transcription 3 (STAT3).

Abstract

The human placenta nourishes and protects the developing fetus whilst influencing maternal physiology for fetal advantage. It expresses several members of the VEGF family including the pro-angiogenic/pro-permeability VEGF-A_{165}a isoform, the anti-angiogenic VEGF-A_{165}b, placental growth factor (PlGF) and their receptors, VEGFR1 and VEGFR2. Alterations in the ratio of these factors during gestation and in complicated pregnancies have been reported; however the impact of this on feto-placental endothelial barrier integrity is unknown. This study investigated the interplay of these factors on junctional occupancy of VE-cadherin and macromolecular leakage in human endothelial monolayers and the perfused placental microvascular bed. Whilst VEGF-A_{165}a (50 ng/ml) increased endothelial monolayer albumin permeability ($p<0.0001$), equimolar concentrations of VEGF-A_{165}b ($p>0.05$) or PlGF ($p>0.05$) did not. Moreover, VEGF-A_{165}b (100 ng/ml; $p<0.001$) but not PlGF (100 ng/ml; $p>0.05$) inhibited VEGF-A_{165}a-induced permeability when added singly. PlGF abolished the VEGF-A_{165}b-induced reduction of VEGF-A_{165}a mediated permeability ($p>0.05$); PlGF was found to compete with VEGF-A_{165}b for binding to Flt-1 at equimolar affinity. Junctional occupancy of VE-cadherin matched alterations in permeability. In the perfused microvascular bed, VEGF-A_{165}b did not induce microvascular leakage but inhibited and reversed VEGF-A_{165}a-induced loss of junctional VE-cadherin and tracer leakage. These results indicate that the anti-angiogenic VEGF-A_{165}b isoform does not increase permeability in human placental microvessels or HUVEC primary cells and can interrupt VEGF-A_{165}a-induced permeability. Moreover, the interplay of these isoforms with PlGF (and s-flt1) suggests that the ratio of these three factors may be important in determining the placental and endothelial barrier in normal and complicated pregnancies.

Introduction

The human placenta is a fetal organ which allows oxygen and selective nutrient uptake from the mother to the fetus, whilst acting as a discriminatory barrier. It does this by having a unique architecture; specific to human and macaque monkeys, where the placental microvessels, encased in a single layer of syncytiotrophoblast, lie bathed in maternal blood (haemomonochorial). Fetal blood enters these vessels through the umbilical arteries and returns replenished via the umbilical vein. Both the thin outer syncytial lining and the fetal endothelium act as resistance in series to transport of hydrophilic solutes from maternal to fetal blood [1]. The feto-placental endothelial barrier integrity is therefore of critical importance to fetal growth and wellbeing.

The placental endothelium is continuous, with well-defined cell-cell junctions that restrict movement of large hydrophilic molecules (>65 kDa) across the paracellular cleft [2]. Adherens junctions (AJs) are the major regulators of paracellular permeability in the placental capillaries with the transmembrane adhesion molecule - Vascular endothelial (VE)-cadherin being the key player [3], [4], [5]. Phosphorylation of VE-cadherin leads to breakage of homophilic binding, loss of anchorage to peri-junctional actin and translocation from AJ domains with accompanying increases in paracellular cleft dimensions and increased paracellular permeability [6]. VEGF-A, via stimulation of VEGFR2 has been shown to increase phosphorylation of VE-Cadherin at Tyr-685 and Tyr-731 facilitating increased solute permeability and extravasation of cells [7].

The human placenta expresses the pro-angiogenic /pro-permeability VEGF-A_{165}a, anti-angiogenic VEGF-A_{165}b, placental growth factor (PlGF) and their receptors, VEGFR2 (KDR), VEGFR1 (Flt-1), neuropilin-1, and soluble Flt-1 (sFlt-

1). There is differential expression of the growth factors during gestation and in complicated pregnancies. VEGF-A levels are highest in the first trimester during de novo synthesis of placental vessels [8, 9]). The in situ location also alters with gestation; in the last trimester VEGF-A is found predominantly in the terminal villi which house dilated fetal capillary loops involved in materno-fetal exchange [10]. Elevated levels of VEGF-A, loss of junctional VE-cadherin and increased vascular leakage have been reported in pregnancies complicated by maternal diabetes ([11], [12] whilst trophoblast derived factors from pre-eclamptic placenta have been shown to diminish barrier function and alter VE-cadherin distribution in vitro [13]. The anti-angiogenic splice variant VEGF-A_{165}b has been shown to be present in human term placentae as a small part of the total VEGF expression. Interestingly, there is a further downregulation of this in pre-eclamptic placenta [14]. Whether this splice-variant can affect placental vascular permeability is not known.

PIGF, a homologue of VEGF [15] rises steadily until the second trimester of pregnancy -a period of maximal vessel maturation and then begins to fall [16]. Lower PIGF levels in maternal circulation have been correlated with small-for-gestational-age babies in normal pregnancies [17] [18]. A down-regulation of syncytiotrophoblast PIGF was found in pre-eclamptic placenta [19]. Its function in the placenta remains to be shown experimentally. Of the various isoforms of PIGF, PIGF-2 is thought to enhance VEGF-induced permeability, whilst PIGF promotes VEGF induced angiogenesis in some models and antagonises in others [20]; [15]).

The interplay of VEGF-A_{165}a, VEGF-A_{165}b and PIGF depend largely on their interactions with their receptors and co-receptors. VEGF-A_{165}a is able to bind to both VEGFR1 and R2 but acts mainly via the latter [21]. Interestingly, neuropilin-

1 can complex with VEGFR1 and R2 and has been shown to potentiate VEGFR2 activation [22]. VEGF-A_{165}b binds to both VEGFR1 and R2 receptors but is a weaker agonist for VEGFR2 [23]. VEGF-A_{165}b differs from VEGF-A_{165}a only in the last six amino acids, the residues necessary for interaction with neuropilin-1, [24] [25] [26] and this lack of co-receptor binding may be behind its function as a partial receptor agonist. PlGF only binds to VEGFR1 but has been shown to propagate kinase cascades for VE-cadherin autophosphorylation [27]. The competitive interplay between the VEGF splice variants and PlGF in regulation of human placental endothelial junctional integrity requires elucidation.

The aim of this study was therefore to investigate whether VEGF-A_{165}a, VEGF-A_{165}b and PlGF, singly or in combination can affect junctional occupancy of VE-cadherin and alter paracellular permeability of human placental/fetal endothelium. Term placenta and umbilical cord from healthy pregnancies were used for ex-vivo placental perfusion experiments and for endothelial primary cell culture studies. Results obtained will further understanding of the mechanisms employed by the human placenta for maintenance of the feto-placental endothelial barrier and how this could be perturbed in complicated pregnancies.

Methodology

Placenta and umbilical cord collection

Term placentas and umbilical cords were obtained at elective Caesarean section from normal pregnancies with informed patient consent and full ethical approval (REC Ref 14/SC/ 1194; NHS Heath Research Authority, UK), and permission from Nottingham University Hospitals, NHS Trust, UK. The work described here has been

carried out in accordance with The Code of Ethics of the World Medical Association (Declaration of Helsinki).

All term placentas and umbilical cords were obtained from term (≥ 37 weeks), non-labouring women undergoing scheduled elective caesarean section delivery. Indications for caesarean section include maternal request, breech presentation, and previous caesarean section. Women with pre-existing conditions such as hypertension (>140/90mmHg), proteinuria, diabetes, gestational diabetes, renal and cardiac disease, and other conditions that may compromise patient health were excluded. Smokers were excluded from the study.

Table 1. Table showing the characteristics of patients undergoing caesarean deliveries who participated in this study, and whose data was used for further analysis.

Age (years)	29.5 ± 4.7
BMI	25.6 ± 2.4
Parity	2 [2 – 3]
Gestational age (weeks)	40.6 ± 3.5
Weight of placenta (g)	701.33 ± 78.5
Sex of offspring:	
Male	37.5%
Female	62.5%
Weight of offspring (kg)	3.3 ± 0.6

(BMI=Body Mass Index; data reported as mean ± the standard deviation (SD), median [Interquartile range (IQR)], or percentage of offspring).

Primary cell culture

Human umbilical vein endothelial cell (HUVECs) were isolated from freshly delivered umbilical cords and cultured on 1% gelatin-coated flasks in complete endothelial cell medium M199 (Gibco), supplemented with 20% foetal bovine serum (FBS), heparin sodium salt (50µg/mL), endothelial cell growth factor supplement (50µg/mL), and penicillin/streptomycin (100U/100mg/mL), under humidified conditions at 37^{o}C and

5% CO_2/95% air. In all experiments, HUVECs were grown and used only up to the third passage.

HUVEC permeability assays

Polyester membrane transwell 6.5mm^2 inserts with a 0.4µm pore diameter (Corning, UK), were coated with 1% gelatin in 0.1M PBS. They were suspended in a 24-well cell culture plates and seeded with 5 x 10^3 cells. 100µL of complete endothelial cell medium M199 was added to the upper compartment and 400µL added to lower compartment to equalise hydrostatic fluid pressures. HUVECs were allowed to form a confluent monolayer before experimentation. There were 4 in built experimental repeats (transwell assays) per experiment. The whole was repeated (x4) using HUVECS isolated from 4 different cords.

Experimental Design

Medium in the upper chamber was replaced with 100µL of dialysed (10kDa dialysis tubing) fluorescein isothiocyanate-conjugated bovine serum albumin (FITC-BSA, 66 kDa; Thermo Fisher) in phenol-free M199 medium at a concentration of 1mg/mL After a 30 min equilibration HUVECs were exposed to a single addition of recombinant human VEGF-A_{165}a (50ng/mL), VEGF-A_{165}b (50ng/mL), or PlGF (50ng/mL). In further experiments, VEGF-A_{165}a (50ng/mL) was followed by VEGF-A_{165}b (100ng/mL), PlGF-2 (264-PG, R&D Systems 100ng/mL) or both VEGF-A_{165}b (100ng/mL) and PlGF-2 (100ng/mL) in combination. 50µL samples were collected from the lower compartment at 0, 30, 60, 90 and 120 minute intervals, with the equivalent volume of fresh phenol-free M199 medium replenished after each sample collection. Samples were diluted in 50µL 0.1M PBS and measured using a Thermo Fluoroskan Ascent F2 fluorescence plate reader at an emission/excitation wavelength of 495/520nm. Concentrations of FITC-albumin in each sample were

calculated via linear regression of a serial dilution series of the tracer. Total permeability of monolayers were calculated for each treatment based on the rate of solute flux (calculated in μg/min) over the first 30 minutes, the surface area of the monolayer, and the initial concentration difference between the upper and lower wells (1mg/ml).

Immunostaining.

After experimentation, monolayers were immediately fixed in 1% PFA. Cells were permeabilised with 0.15% Triton X-100 followed by blocking with 4% normal human serum in 0.1M PBS for 30 minutes at RT. Monolayers were incubated with mouse anti-human CD144 (ThermoFisher) (VE-cadherin; 5μg/mL) overnight at 4^{o}C and FITC-conjugated goat anti-mouse IgG (Sigma-Aldrich, 20μg/mL) for 2 hours at 37^{o}C in the dark after requisite washes.

Extra-corporeal perfusion of the placental microvascular bed

A well-established dual-perfusion procedure was employed [1,2, 9-12]. To summarise, immediately after Caesarean delivery, the placenta was transferred to a 37°C chamber with the umbilical cord kept clamped until cannulation to prevent loss of blood and collapse of feto-placental vessels. Within 20 min of arrival of the placenta, a vein and an artery supplying the microvascular bed of a randomly chosen intact cotyledon were each cannulated with a nasogastric (5mm) tube to establish the fetal circulation. The placenta was inverted and the cotyledon was clamped in a Perspex chamber to isolate the lobule from the rest of the placenta. The independent maternal circulation was simulated by inserting five 5mm nasogastric tubes into the intervillous space through the basal plate of the cotyledon, and drained through an exit tube in the Perspex chamber. Fetal and maternal circulations were connected to

peristaltic pumps providing a constant 20ml/min flow to the maternal circulation and a 5ml/min flow to the fetal circulation, replicating the physiologic flow rates seen *in utero*. Establishment of both circulations were completed within 30 minutes of delivery to minimize hypoxic damage to the placenta. Perfusion was abandoned if fetal venous outflow was less than arterial inflow. From the 20 intact placenta recruited for the perfusion experiments, 15 allowed full perfusion (25% failure rate).

Experimental Design

A 20 minute open circuit equilibration period with oxygenated Medium 199 (Sigma, Poole, UK), with added sodium bicarbonate (2.2g/l), albumin (5g/l), high molecular weight dextran (20,00 Mr; 8g/l) and heparin (5000IU/l) (final pH 7.2 to 7.4), was performed to reverse any post-parturition hypoxic changes [1]. After equilibration, fetal oxygenation was discontinued and both the maternal and fetal circulations were closed. Perfusion pressures were monitored and accepted if fetal pressure was between 40-80mmHg and maternal pressure was between 18-20mmHg [2].

Recombinant human VEGF-A_{165}a (20ng/mL), VEGF-A_{165}b (20ng/mL) or vehicle was introduced into the fetal circulation and the lobules perfused for 30 minutes. In reversal experiments, VEGF-A_{165}a exposure was followed by a separate VEGF-A_{165}b (40ng/mL) perfusion (vehicle only acted as control) for an additional 30 mins. Three different placenta was used for each experimental exposure. Tetramethylrhodamine isothiocyanate (TRITC)-conjugated dextran (76 M_r; Sigma, Dorset, U.K), 1mg/mL) was added as a bolus into the fetal circulation for the last 10 minutes of all perfusions (single growth factors or sequential VEGF isoform perfusions). The lobules were then perfusion fixed with 1% paraformaldehyde in 0.1M phosphate buffer saline (pH 7.3) for 30 minutes. The lobule was excised and 10mm^3 biopsies taken for a further immersion fixation (2h). Biopsies were rinsed in

PBS, cut into 5mm^3 pieces, frozen in nitrogen-cooled isopentane (Fisher Scientific UK Limited, Loughborough, U.K) and stored at -80°C until required.

Immunostaining.

A minimum of 6 different blocks (randomly chosen) per placenta were cryosectioned and a minimum of 6 sections (5µm thick) were taken from each block at different depths. Cryo-sections were air-dried and washed in 0.1M PBS/BSA, before permeabilisation with 0.15% Triton X-100 followed by blocking with 4% normal human serum in 0.1M PBS for 30 minutes at room temperature. Sections were incubated overnight with mouse anti-human CD144 (VE-cadherin; 5µg/mL) at 4^{o}C and secondary antibodies as described before.

Microscopy and analysis

Transwell membranes and placental sections were visualised for expression of CD144 and TRITC-Dextran tracer using a Nikon LaboPhot-2 fluorescence microscope (Nikon, UK) and appropriate TRITC/FITC filters. Images (obtained by systematic random sampling of entire sections or membranes) from both channels were acquired using a Nikon Coolpix 995 camera (Nikon, UK).

Junctional integrity and tracer leakage analysis

Micrographs were analysed using Adobe Photoshop 6.0 (Adobe systems, UK). A pre-determined electronic grid was placed over each image and both VE-cadherin junction integrity and evidence of TRITC-Dextran tracer leakage quantified using systematic random sampling and unbiased 'forbidden line' counting principle to ensure that no vascular profile and paracellular cleft was counted twice [11]. For sampling efficiency a minimum of 200 vascular profiles were counted from images

per perfused placenta; c 600 vascular profiles were analysed for each experimental condition. For HUVEC monolayers, junctional integrity was determined by counting the % of paracellular clefts showing uniform VE-cadherin staining as a continuous thin line. Gaps in cell-cell adhesion regions with VE-cadherin negative cell edges were also counted. The % of cell-cell overlap showing thicker bands of VE-cadherin localisation was noted. For placental sections, the total percentage of vascular profiles showing disrupted junctional VE-cadherin (discontinuous staining or total loss) from paracellular clefts and associated tracer leakage (76 M_r Dextran-TRITC visualised as peri-vascular ablumenal fluorescent puncta or 'hot-spots') were counted [11]. All experimental images from both HUVEC monolayers and placental sections were blinded to treatment regime before analyses.

Competitive binding ELISA

High-attachment 96-well ELISA plates (Corning, UK) were coated with recombinant Flt-1 overnight, and co-incubated with biotinylated-VEGF-A_{165}b (EC75), followed by non-biotinylated-VEGF-A_{165}a (0 – 160nM or PlGF (0 – 160nM). Differences in VEGF binding to Flt-1 (n=12) were measured using streptavidin-HRP to biotin interactions, using a Thermo Fluoroskan Ascent F2 fluorescence plate reader at an absorbance wavelength of 450nm.

Statistical Analyses

All Statistical Analysis was carried out using Graphpad Prism. Comparisons of means were made using one way ANOVA with Bonferroni's post hoc test.

Results

VEGF-A_{165}b inhibits VEGF-A_{165}a-mediated permeability in HUVECs

Incubation of HUVEC monolayers with VEGF-A_{165}a resulted in an increase in FITC-albumin tracer mass leakage over time (Figure 1A) compared to vehicle exposed cells. In contrast, incubation with VEGF-A_{165}b in isolation showed no change in FITC-albumin tracer mass permeate compared to vehicle over time. Co-incubation of VEGF-A_{165}b following 30 mins of VEGF-A_{165}a exposure resulted in the inhibition of VEGF-A_{165}a-mediated increase in FITC-albumin tracer mass leak (Figure 1A).

Exposure to PlGF alone also resulted in no change in FITC-albumin tracer mass permeate with time (Figure 1B). Addition of PlGF after 30 min exposure to VEGF-A_{165}a did not prevent the VEGF-A_{165}a-mediated effects (See Figure 1B). Addition of PlGF alongside VEGF-A_{165}b prevented VEGF-A_{165}b-induced inhibition of VEGF-A_{165}a-mediated increase in FITC-albumin tracer mass leak (See Figure 1C). The calculated permeability values to FITC-albumin tracer reflected these observations, whereby exposure to VEGF-A_{165}a, but not VEGF-A_{165}b or PlGF significantly increased HUVEC monolayer permeability ($P<0.001$, Figure 1D). Similarly, VEGF-A_{165}a-mediated permeability increase was inhibited by VEGF-A_{165}b ($P<0.001$) but not PlGF ($P>0.05$). PlGF co-incubation with VEGF-A_{165}b abolished the rescue of the latter from VEGF-A_{165}a dependent increases in permeability ($P<0.001$) (Figure 1D).

VEGF-A_{165}a but not VEGF-A_{165}b or PlGF disrupts VE-cadherin junctions in HUVECs

VE-Cadherin immunostaining demonstrated the presence of positive junctional cell-cell overlap regions and thin abutting junctions with continuous VE-cadherin staining (Figure 2) in control (vehicle only) experiments. Monolayers treated with VEGF-A_{165}a revealed observable endothelial junctional disruption after exposure (Figure 2B) with a decrease in continuous thin junctions and increase in discontinuities or total loss of

VE-cadherin staining in cell-cell margins (described as gaps). This was not seen when monolayers were treated with VEGF-A_{165}b (Figure 2C) or PlGF (Figure 2D). Quantification (systematic random sampling) of the percentage of each type of VE-cadherin positive regions (Figure 2H) showed that there was a statistically significant decrease in the number of thin junctions showing continuous VE-cadherin occupancy ($P<0.0001$) after VEGF-A_{165}a exposure. VE-cadherin discontinuity within paracellular clefts increased with a significant increase in observable gaps ($P<0.001$). No significant change in both percentage of disrupted junctions and % of continuous VE-cadherin junctions were found in VEGF-A_{165}b or PlGF experiments when compared to controls ($P>0.05$, Figure 2H).

VEGF-A_{165}b prevented VEGF-A_{165}a-mediated VE-cadherin junctional disruption, which was inhibited by PlGF

VEGF-A_{165}b (Figure 2E), but not PlGF (Figure 2F) was able to prevent VEGF-A_{165}a-induced disruption of VE-cadherin junctions after 2 hours exposure. However, addition of PlGF in combination with VEGF-A_{165}b (Figure 2G) prevented the observed VEGF-A_{165}b-mediated inhibition of VEGF-A_{165}a-induced junctional disruption. Analysis of percentage junctional integrity (Figure 2I) revealed a significant decrease in percentage of gaps after VEGF-A_{165}b co-incubation ($P<0.0001$) and an increase in percentage of thin continuous VE-cadherin junctions ($P<0.01$). No significant change in either percentage gap or continuous VE-cadherin AJ staining were observed after PlGF co-incubation ($P>0.05$). However, PlGF exposure in combination with VEGF-A_{165}b abolished the VEGF-A_{165}b inhibition of VEGF-A_{165}a mediated effects ($P>0.05$) (See Figure 2I).

PlGF competes with VEGF-A_{165}b for binding to Flt-1

As the VEGF-A_{165}b inhibition of VEGF-A_{165}a mediated increased permeability, was blocked by PlGF, which only binds VEGFR1 (flt-1), we hypothesised that this could occur if VEGF-A_{165}b was inhibiting VEGF-A_{165}a by signalling through VEGFR1. VEGF-A_{165}a and VEGF-A_{165}b compete for R1 [28], so we therefore determined the effect of PlGF on VEGF-A_{165}b binding to VEGFR1 using an Fc-VEGFR1 chimeric protein. Incubation of Fc-VEGFR1 with un-labelled human recombinant VEGF-A_{165}b resulted in a concentration dependent decrease in binding of biotinylated-VEGF-A_{165}b (EC75). Similarly, co-incubation with un-labelled PlGF resulted in an almost identical concentration dependent decrease in biotinylated-VEGF-A_{165}b binding, with no significant difference in calculated IC_{50} between the two proteins ($P>0.05$) (See Figure 3), thus suggesting that the inhibition of VEGF-A_{165}a mediated permeability by VEGF-A_{165}b could also be through its actions on VEGFR1.

VEGF-A_{165}a-mediated increased permeability and VE-cadherin disruption is prevented by VEGF-A_{165}b in the perfused human placental microvascular bed

Using the more physiological dual perfusion system, addition of growth factors to the fetal microcirculation of term placental lobules resulted in observable differences in extravasation of TRITC-dextran ($75M_r$) tracer (See Figure 4, right panel). VEGF-A_{165}a perfusions for 30 min resulted in a significant increase in percentage of vascular profiles associated with tracer leakage (71.2 ± 13.8%, Figure 4, 5) compared with control perfusions (30.2 ± 4.4%; $P<0.01$). In contrast, perfusions of VEGF-A_{165}b saw no significant increase in percentage of leaky vessels ($P>0.05$) compared to control perfusions. Addition of VEGF-A_{165}b into the closed fetal circulation after a 30 min VEGF-A_{165}a perfusion period resulted in altered tracer

leakage profile from that obtained with VEGF-A_{165}a only perfusions. 9.4 ± 1.2% vascular profiles were now found to be associated with peri-vascular 'hot-spots' ($P<0.05$). This was not due to temporal recovery, as addition of vehicle only for 30 min after VEGF-A_{165}a perfusion showed no significant decrease in profiles expressing hot spots ($p> 0.05$). Subsequent immunohistochemical analyses of the same sections revealed that tracer leakage matched disruption of VE-cadherin AJs (loss of VE-cadherin from paracellular clefts) (Figure 4, left panel). VEGF-A_{165}a-perfusion of placental microvascular beds resulted in a 49.3% decrease in vascular profiles showing VE-cadherin at paracellular clefts ($P<0.01$), while perfusions of VEGF-A_{165}b did not significantly alter VE-cadherin positive vascular profiles (86.7 ± 0.8%) compared with controls (89.3 ± 2.3%) ($P>0.05$). Sequential addition of VEGF-A_{165}b to VEGF-A_{165}a perfusions resulted in a recovery of junctional integrity with 81 ± 5% of vascular profiles showing VE-cadherin at paracellular clefts ($P<0.05$; Figure 5).

Discussion

These studies are the first to show that the anti-angiogenic VEGF-A_{165}b does not disturb the junctional occupancy of VE-cadherin or induce paracellular tracer leakage in the human placental microvascular bed and HUVEC monolayers. Indeed, VEGF-A_{165}b (at a twofold concentration) can block/reverse VEGF-A_{165}a-mediated increases in feto-placental endothelial permeability to macromolecules (75 kDa) and loss of VE-cadherin from AJs. In these experiments, PlGF did not affect endothelial integrity, VE-cadherin localisation and permeability when added singly, however it could prevent the rescue of VEGF-A_{165}a-mediated effects by VEGF-A_{165}b.

The similarities between the observed induced changes in both fetal endothelial cell cultures and the more physiological and complex perfused microvascular bed is re-assuring. Placental microvessels showed a robust response to a 30 min perfusion of exogenous VEGF-A_{165}a, with loss of VE-cadherin and increased vascular leak of 76kDa dextrans. These changes were not induced when microvessels were perfused with VEGF-A_{165}b; indeed this splice variant could reverse the VEGF-A_{165}a induced changes both in the perfusion model and in transwell experiments.

The monolayer permeability results are similar to those recently described in lung pulmonary endothelial cells [29], where VEGF-A_{165}a but not VEGF-A_{165}b was shown to increase monolayer permeability and decrease junctional integrity. However, they did not investigate the effect of PlGF on these cells.

The observed inability of either PlGF or VEGF-A_{165}b to alter VE-cadherin occupancy and AJ integrity in human placental microvessels and fetal endothelial cells may be due to their lack of neuropilin-1 binding property [30] [22] [26]. Neuropilin-1 is critical for VEGF-mediated endothelial permeability in human pulmonary endothelial cells and for pulmonary vascular leaks in inducible lung-specific VEGF transgenic mice [22]. Stable transfection of the neuropilin-1/VEGFR2 complex in endothelial cells resulted in decreased transendothelial resistance in a dose-dependent fashion following addition of VEGF-A_{165}a; this was not seen for single transfections of VEGFR2 or neuropilin-1 alone. Moreover, VEGF-A_{165}b prevents the formation of neuropilin-VEGFR2 complexes by VEGF-A_{165}a [31]. The reduction of VEGF-A_{165}a-mediated enhanced permeability in our studies, may be due to competitive binding of VEGF-A_{165}b to the VEGFR2 receptor [25]. KDR occupancy by VEGF-A_{165}b may be followed by internalisation but not the subsequent neuropilin-1 dependent re-shuttling of KDR to the membrane surface [32]. This therefore would rule out further

VEGF-A_{165}a binding and triggering of phosphorylation events that lead to translocation of VE-cadherin from AJ domains. The recovery of junctional integrity seen in the sequential VEGF-A_{165}a + VEGF-A_{165}b perfusions, but not in VEGF-A_{165}a + vehicle perfusions argues that VEGF-A_{165}b is acting as an active signalling inhibitor. Our data allows one to hypothesise that the relative contributions of the two different VEGF-A_{165} isoforms may be an important driver behind the different feto-placental vascular permeability (and angiogenesis) observed for the different trimesters of pregnancy [9, 10].

Plasma taken from pre-eclamptic mothers has been shown to induce transient increases in permeability in amphibian models, which was blocked by VEGF-A_{165}b specific neutralising antibodies, and receptor tyrosine inhibitors at concentrations specific to VEGFR1 blockage [33]. This neutralising antibody to VEGF-A_{165}b was shown to prevent the inhibition of VEGF-A_{165}b-mediated blockade of VEGF-A_{165}a-induced migration and cytoprotection of endothelial cells [34] and anti-angiogenesis in peripheral vascular disease [35]. This suggests that the pre-eclamptic plasma contained not only physiologically active VEGF-A_{165}b, but that its action was incurred by altering the balance of VEGF-A_{165}b, PlGF and VEGF-A_{165}a, such that VEGF-A_{165}a was no longer able to induce the increase in permeability, potentially by binding heterodimers of VEGF-A_{165}b with either PlGF or VEGF-A_{165}a. Such heterodimers are theoretically possible but have not yet been clearly demonstrated.

PlGF did not increase AJ disruption or permeability of the fetal human umbilical vein endothelial cells. PlGF-1, but not PlGF-2, has been shown to stabilise VE-cadherin junctions after activation with VEGF in bovine retinal endothelial cells and after intra-vitreal injections in mouse, during a critical window [36]. The isoform used here was PlGF-2, which binds heparin and is therefore able to signal through VEGFR1 with

heparin, indicating that full signalling does require the heparin binding domains. The PlGF mediated abolition of VEGF-A_{165}b induced reversal of VEGF-A_{165}a induced permeability was surprising. However, recent studies by Ganta et al., [37] have shown that VEGF-A_{165}b inhibits VEGF-A_{165}a mediated signalling in adipose endothelial cells through inhibiting VEGFR1 mediated activation of the STAT3 pathway. It is therefore possible that VEGF-A_{165}b binds VEGFR1, inhibiting STAT3 signalling. When PlGF binds VEGFR1, if it does not inhibit STAT3 signalling (or stimulates it), and prevents VEGF-A_{165}b from inhibiting it, so VEGF-A_{165}a would then be at liberty to increase permeability. There are currently no studies identifying whether PlGF signals through STAT3, nor how it impacts on VEGF-A_{165}a mediated STAT3 signalling, but it would appear that such studies are warranted.

In our HUVEC studies, when PlGF was added in combination with VEGF-A_{165}b, there was an abolition of the VEGF-A_{165}b induced reversal of VEGF-A_{165}a- induced permeability. Whilst it is well known that VEGF-A_{165}a and PlGF can compete for VEGF-R1 binding [38], in this study we have also shown that incubation of Fc-VEGFR1 with un-labelled PlGF resulted in a concentration dependent decrease in biotinylated-VEGF-A_{165}b binding. Thus addition of PlGF may have resulted in release of both splice variants. The excess VEGF-A_{165}a would then be at liberty to increase permeability via KDR-(neuropilin) signalling. Hetero-dimerization of PlGF with VEGF-A_{165}b could further assist VEGF-A_{165}a activity. Further studies are needed to understand the complex interplay between VEGF-A/PlGF and their receptors/co-receptors. Elucidation of the multiple signalling pathways, including whether/where the VEGFR1 linked angiogenic signalling pathway interacts with the VEGFR2 linked phosphorylation events that lead to disruption of VE-cadherin junctions is needed to understand how placental/fetal barrier function is regulated.

In summary we have shown that VEGF-A_{165}b is able to inhibit vascular permeability induced by VEGF-A_{165}a in vitro, and in human placenta ex vivo, and that this is interfered with by placental growth factor. These results suggests that alterations in the ratio of these growth factors during normal placental development and in complicated pregnancies such as pre-eclampsia and diabetes would influence VE-cadherin clustering in fetal vessels and therefore placental barrier function, given that both the fetal endothelium and the syncytiotrophoblast act as resistance in series to materno-fetal hydrophilic solute transport.

CLINICAL PERSPECTIVES

- The anti-angiogenic VEGF-A_{165}b isoform does not increase permeability in human placental microvessels or fetal endothelial cells.
- VEGF-A_{165}b isoform can interrupt VEGF-A_{165}a-induced permeability of feto-placental vessels.
- The interplay of the VEGF-A_{165} isoforms with PlGF suggests that the ratio of these three factors may be important in determining the placental endothelial barrier and therefore fetal well-being in normal and complicated pregnancies.

ACKNOWLEDGEMENTS

This work was supported by BHF grant number PG/13/85/30536. We would like to thank clinical staff and midwives at the Labour Ward, Queens Medical Centre, Nottingham University Hospital for the timely retrieval of placenta.

CONFLICT OF INTEREST

The authors declare they have no conflict of interests.

AUTHOR CONTRIBUTIONS

Vincent Pang performed most of the experiments, statistical analyses and was involved in writing the manuscript. Lopa Leach and Dave Bates co-designed and co-directed the study and was involved in manuscript writing. Lopa Leach assisted with the placental perfusions, directed analyses of the tracer leakage and VE-cadherin dynamics. All authors reviewed the manuscript.

References

1 Leach, L. and Firth, J. A. (1992) Fine structure of the paracellular junctions of terminal villous capillaries in the perfused human placenta. Cell Tissue Res. **268**, 447-452

2 Eaton, B. M., Leach, L. and Firth, J. A. (1993) Permeability of the fetal villous microvasculature in the isolated perfused term human placenta. J Physiol (Lond). **463**, 141-155

3 Leach, L., Clark, P., Lampugnani, M. G., Arroyo, A. G., Dejana, E. and Firth, J. A. (1993) Immunoelectron characterisation of the inter-endothelial junctions of human term placenta. J Cell Sci. **104 (Pt 4)**, 1073-1081

4 Dejana, E., Orsenigo, F. and Lampugnani, M. G. (2008) The role of adherens junctions and VE-cadherin in the control of vascular permeability. J Cell Sci. **121**, 2115-2122

5 Gavard, J. (2013) Endothelial permeability and VE-cadherin: a wacky comradeship. Cell adhesion & migration. **7**, 455-461

6 Esser, S., Lampugnani, M. G., Corada, M., Dejana, E. and Risau, W. (1998) Vascular endothelial growth factor induces VE-cadherin tyrosine phosphorylation in endothelial cells. J Cell Sci. **111 (Pt 13)**, 1853-1865

7 Wessel, F., Winderlich, M., Holm, M., Frye, M., Rivera-Galdos, R., Vockel, M., Linnepe, R., Ipe, U., Stadtmann, A., Zarbock, A., et al. (2014) Leukocyte extravasation and vascular permeability are each controlled in vivo by different tyrosine residues of VE-cadherin. Nat Immunol. **15**, 223-230

8 Demir, R., Seval, Y. and Huppertz, B. (2007) Vasculogenesis and angiogenesis in the early human placenta. Acta histochemica. **109**, 257-265

9 Leach, L., Babawale, M. O., Anderson, M. and Lammiman, M. (2002) Vasculogenesis, angiogenesis and the molecular organisation of endothelial junctions in the early human placenta. J Vasc Res. **39**, 246-259

10 Leach, L., Lammiman, M. J., Babawale, M. O., Hobson, S. A., Bromilou, B., Lovat, S. and Simmonds, M. J. (2000) Molecular organization of tight and adherens junctions in the human placental vascular tree. Placenta. **21**, 547-557

11 Leach, L., Gray, C., Staton, S., Babawale, M. O., Gruchy, A., Foster, C., Mayhew, T. M. and James, D. K. (2004) Vascular endothelial cadherin and beta-catenin in human fetoplacental vessels of pregnancies complicated by Type 1

diabetes: associations with angiogenesis and perturbed barrier function. Diabetologia. **47**, 695-709
12 Babawale, M. O., Lovat, S., Mayhew, T. M., Lammiman, M. J., James, D. K. and Leach, L. (2000) Effects of gestational diabetes on junctional adhesion molecules in human term placental vasculature. Diabetologia. **43**, 1185-1196
13 Wang, Y., Lewis, D. F., Gu, Y., Zhang, Y., Alexander, J. S. and Granger, D. N. (2004) Placental trophoblast-derived factors diminish endothelial barrier function. J Clin Endocrinol Metab. **89**, 2421-2428
14 Bates, D. O., MacMillan, P. P., Manjaly, J. G., Qiu, Y., Hudson, S. J., Bevan, H. S., Hunter, A. J., Soothill, P. W., Read, M., Donaldson, L. F., et al. (2006) The endogenous anti-angiogenic family of splice variants of VEGF, VEGFxxxb, are down-regulated in pre-eclamptic placentae at term. Clin Sci (Lond). **110**, 575-585
15. Carmeliet, P., Moons, L., Luttun, A., Vincenti, V., Compernolle, V., De Mol, M., Wu, Y., Bono, F., Devy, L., Beck, H., et al. (2001) Synergism between vascular endothelial growth factor and placental growth factor contributes to angiogenesis and plasma extravasation in pathological conditions. Nat Med. **7**, 575-583.
16 Levine, R. J., Maynard, S. E., Qian, C., Lim, K. H., England, L. J., Yu, K. F., Schisterman, E. F., Thadhani, R., Sachs, B. P., Epstein, F. H., et al. (2004) Circulating angiogenic factors and the risk of preeclampsia. N Engl J Med. **350**, 672-683
17 Benton, S. J., Hu, Y., Xie, F., Kupfer, K., Lee, S. W., Magee, L. A. and von Dadelszen, P. (2012) Can placental growth factor in maternal circulation identify fetuses with placental intrauterine growth restriction? Am J Obstet Gynecol. **206**, 163 e161-167
18 Benton, S. J., McCowan, L. M., Heazell, A. E., Grynspan, D., Hutcheon, J. A., Senger, C., Burke, O., Chan, Y., Harding, J. E., Yockell-Lelievre, J., et al. (2016) Placental growth factor as a marker of fetal growth restriction caused by placental dysfunction. Placenta. **42**, 1-8
19 Mizuuchi, M., Cindrova-Davies, T., Olovsson, M., Charnock-Jones, D. S., Burton, G. J. and Yung, H. W. (2016) Placental endoplasmic reticulum stress negatively regulates transcription of placental growth factor via ATF4 and ATF6beta: implications for the pathophysiology of human pregnancy complications. J Pathol. **238**, 550-561
20 Eriksson, A., Cao, R., Pawliuk, R., Berg, S. M., Tsang, M., Zhou, D., Fleet, C., Tritsaris, K., Dissing, S., Leboulch, P., et al. (2002) Placenta growth factor-1 antagonizes VEGF-induced angiogenesis and tumor growth by the formation of functionally inactive PlGF-1/VEGF heterodimers. Cancer Cell. **1**, 99-108
21 Bates, D. O. and Harper, S. J. (2002) Regulation of vascular permeability by vascular endothelial growth factors. Vascul Pharmacol. **39**, 225-237
22 Becker, P. M., Waltenberger, J., Yachechko, R., Mirzapoiazova, T., Sham, J. S., Lee, C. G., Elias, J. A. and Verin, A. D. (2005) Neuropilin-1 regulates vascular endothelial growth factor-mediated endothelial permeability. Circ Res. **96**, 1257-1265
23. Kawamura, H., Li, X., Harper, S. J., Bates, D. O. and Claesson-Welsh, L. (2008) Vascular endothelial growth factor (VEGF)-A165b is a weak in vitro agonist for VEGF receptor-2 due to lack of coreceptor binding and deficient regulation of kinase activity. Cancer Res. **68**, 4683-4692
24 Bates, D. O., Cui, T. G., Doughty, J. M., Winkler, M., Sugiono, M., Shields, J. D., Peat, D., Gillatt, D. and Harper, S. J. (2002) VEGF165b, an inhibitory splice variant of vascular endothelial growth factor, is down-regulated in renal cell carcinoma. Cancer Res. **62**, 4123-4131.

25 Woolard, J., Wang, W. Y., Bevan, H. S., Qiu, Y., Morbidelli, L., Pritchard-Jones, R. O., Cui, T. G., Sugiono, M., Waine, E., Perrin, R., et al. (2004) VEGF165b, an inhibitory vascular endothelial growth factor splice variant: mechanism of action, in vivo effect on angiogenesis and endogenous protein expression. Cancer Res. **64**, 7822-7835
26 Cebe Suarez, S., Pieren, M., Cariolato, L., Arn, S., Hoffmann, U., Bogucki, A., Manlius, C., Wood, J. and Ballmer-Hofer, K. (2006) A VEGF-A splice variant defective for heparan sulfate and neuropilin-1 binding shows attenuated signaling through VEGFR-2. Cell Mol Life Sci. **63**, 2067-2077

.

27 Autiero, M., Luttun, A., Tjwa, M. and Carmeliet, P. (2003) Placental growth factor and its receptor, vascular endothelial growth factor receptor-1: novel targets for stimulation of ischemic tissue revascularization and inhibition of angiogenic and inflammatory disorders. Journal of thrombosis and haemostasis : JTH. **1**, 1356-1370
28 Hua, J., Spee, C., Kase, S., Rennel, E. S., Magnussen, A. L., Qiu, Y., Varey, A., Dhayade, S., Churchill, A. J., Harper, S. J., et al. (2010) Recombinant human VEGF165b inhibits experimental choroidal neovascularization. Invest Ophthalmol Vis Sci. **51**, 4282-4288
29 Ourradi, K., Blythe, T., Jarrett, C., Barratt, S. L., Welsh, G. I. and Millar, A. B. (2017) VEGF isoforms have differential effects on permeability of human pulmonary microvascular endothelial cells. Respiratory research. **18**, 116
30 Migdal, M., Huppertz, B., Tessler, S., Comforti, A., Shibuya, M., Reich, R., Baumann, H. and Neufeld, G. (1998) Neuropilin-1 is a placenta growth factor-2 receptor. J Biol Chem. **273**, 22272-22278
31 Delcombel, R., Janssen, L., Vassy, R., Gammons, M., Haddad, O., Richard, B., Letourneur, D., Bates, D., Hendricks, C., Waltenberger, J., et al. (2013) New prospects in the roles of the C-terminal domains of VEGF-A and their cooperation for ligand binding, cellular signaling and vessels formation. Angiogenesis. **16**, 353-371
32 Ballmer-Hofer, K., Andersson, A. E., Ratcliffe, L. E. and Berger, P. (2011) Neuropilin-1 promotes VEGFR-2 trafficking through Rab11 vesicles thereby specifying signal output. Blood
33 Bills, V. L., Salmon, A. H., Harper, S. J., Overton, T. G., Neal, C. R., Jeffery, B., Soothill, P. W. and Bates, D. O. (2011) Impaired vascular permeability regulation caused by the VEGF(1)(6)(5)b splice variant in pre-eclampsia. BJOG. **118**, 1253-1261
34 Magnussen, A. L., Rennel, E. S., Hua, J., Bevan, H. S., Beazley Long, N., Lehrling, C., Gammons, M., Floege, J., Harper, S. J., Agostini, H. T., et al. (2010) VEGF-A165b is cytoprotective and antiangiogenic in the retina. Invest Ophthalmol Vis Sci. **51**, 4273-4281
35 Kikuchi, R., Nakamura, K., MacLauchlan, S., Ngo, D. T., Shimizu, I., Fuster, J. J., Katanasaka, Y., Yoshida, S., Qiu, Y., Yamaguchi, T. P., et al. (2014) An antiangiogenic isoform of VEGF-A contributes to impaired vascularization in peripheral artery disease. Nat Med
36 Cai, J., Wu, L., Qi, X., Shaw, L., Li Calzi, S., Caballero, S., Jiang, W. G., Vinores, S. A., Antonetti, D., Ahmed, A., et al. (2011) Placenta growth factor-1 exerts time-dependent stabilization of adherens junctions following VEGF-induced vascular permeability. PLoS One. **6**, e18076

37 Ganta, V. C., Choi, M., Kutateladze, A. and BH, A. (2017) VEGF165b modulates endothelial VEGFR1-STAT3 signaling pathway and angiogenesis in human and experimental peripheral arterial disease Circ Res. **in press**
38 Park, J. E., Chen, H. H., Winer, J., Houck, K. A. and Ferrara, N. (1994) Placenta growth factor. Potentiation of vascular endothelial growth factor bioactivity, in vitro and in vivo, and high affinity binding to Flt-1 but not to Flk-1/KDR. J Biol Chem. **269**, 25646-25654

Figure Legends

Figure 1. VEGF-A_{165}b inhibits VEGF-A_{165}a mediated permeability increase in HUVEC monolayers.

Graphs showing accumulation of FITC-albumin over time in transwell experiments (**A,B,C**) following exposure to VEGF-A_{165} isoforms, PlGF and vehicle only. Single VEGF additions were added at time=0. Arrows indicate time of addition of VEGFs. (**A**) VEGF-A_{165}a (n=9, red trace) showing increase in tracer mass leakage over time compared to vehicle exposed cells (black). VEGF-A_{165}b (blue) shows similar leakage trace as vehicle. Addition of VEGF-A_{165}b (n=11) following 30 mins of VEGF-A_{165}a exposure resulted in inhibition of this (green). (**B**) PlGF alone (n=7, magenta trace) did not increase tracer leakage, whilst co-incubation with VEGF-A_{165}a (orange) shows no inhibition of its activity (red). (**C**) Combination of all three growth factors (n=5, olive) shows increased FITC-albumin solute flux, similar to VEGF-A_{165}a alone. (**D**) Histograph showing the calculated permeability values of the HUVEC monolayers. VEGF-A_{165}a-mediated HUVEC permeability was inhibited by addition of VEGF-A_{165}b but not PlGF (X-axis). Co-incubation of PlGF with VEGF-A_{165}b abolished the VEGF-A_{165}b inhibition of VEGF-A_{165}a-dependent increase in permeability (***=$P<0.001$ compared to vehicle). ND=not determined.

Figure 2. VEGF-A_{165}b inhibits VEGF-A_{165}a induced disruption of VE-cadherin junctions.

A-D. Fluorescent micrographs showing VE-Cadherin (green) immunolocalisation in HUVEC monolayers treated with single additions of VEGF splice variants, PlGF or vehicle**.** (**A**) In control monolayers (vehicle treated) VE-cadherin was visualised as thick staining in cell-cell overlap regions (red arrow; thick junctions) and as continuous thin lines (yellow arrow) between cells. Some cell-cell boundaries revealed discontinuous staining (white arrow) or extensive loss of VE-cadherin staining (asterisk). Nuclei were stained with PI (red). (**B**) Monolayers treated with VEGF-A_{165}a showed increased numbers of cell-cell junctions with loss of or discontinuous VE-cadherin staining. This increase was not seen in monolayers exposed to VEGF-A_{165}b (**C**) or PlGF (**D**).

E-G. Fluorescent micrographs showing VE-Cadherin immunostaining in HUVEC monolayers incubated with VEGF-A_{165}a and VEGF-A_{165}b (**E**) or PlGF (**F**) or both VEGF-A_{165}b + PlGF (**G**). VE-cadherin was found to show a continuous pattern of VE-cadherin staining similar to control (see **A**) when co-incubated with VEGF-A_{165}b (**E**). Disruption of VE-cadherin staining was observed in monolayers co-incubated with PlGF (**F**). Incubation with all three growth factors (**G**) resulted in persistence of discontinuous junctional profiles (asterisk, white arrows) seen for VEGF-A_{165}a alone. Bar = 50μm.

H, I. Quantitative analyses of VE-cadherin junctional occupancy after exposure to growth factors.

(H). 2 h exposure to VEGF-A_{165}a (n=5) resulted in an increase in the percentage of junctions showing discontinuous or loss of junctional VE-cadherin (gaps, ***=P<0.001) and decrease in the percentage of thin continuous VE-cadherin

junctions (****=P<0.0001) when compared to vehicle only study group. Both VEGF-A_{165}b (n=5) and PlGF (n=3) exposure did not change percentage junction integrity when compared to vehicle (p>0.05). The number of overlapping cell-cell regions (thick) were not found to be statistically different for the different treatments.

(**I**). VEGF-A_{165}b co-incubation with VEGF-A_{165}a (n=5) decreased the percentage of junctions showing gaps (****=P<0.0001) and increased the percentage of continuous VE-cadherin thin junctions (**=P<0.01) compared to VEGF-A_{165}a. This was not seen in the PlGF co-incubation experimental group (n=3). However, PlGF in combination with VEGF-A_{165}b (n=3) abolished VEGF-A_{165}b inhibition of VEGF-A_{165}a mediated effects.

Figure 3. PlGF competes with VEGF-A_{165}b for binding to Flt-1.

Co-incubation of Fc-VEGFR1 with un-labelled VEGF-A_{165}b resulted in decreased binding of biotinylated-VEGF-A_{165}b (n=4). PlGF co-incubation equally inhibited biotinylated-VEGF-A_{165}b binding to Flt-1 binding (n=4) (ns=P>0.05)

Figure 4. VEGF-A_{165}b reverses VEGF-A_{165}a induced loss of junctional VE-cadherin and increased tracer leakage in perfused placental microvessels.

Representative fluorescent micrographs of villous biopsies taken from perfused placental microvascular beds . Left panel shows VE-cadherin staining (FITC filter) whilst right panel shows the same image under TRITC filter to visualise any peri-vascular TRITC-dextran “hotspots”. Bar = 100 µm.

A. Image from **c**ontrol perfusion (vehicle only for 30 min) showing VE-cadherin positive microvascular profiles within placental villous trees. **B.** No peri-vascular hot spots can be seen in the same villous trees. **C.** Image showing a dramatic reduction

in VE-cadherin positive vascular profiles following a 30 min perfusion with VEGF-A_{165}a. **D**. Numerous tracer hot spots can now be seen trapped in the peri-vascular regions. **E.** Image showing numerous VE-cadherin positive microvascular profiles in villous trees following perfusion with VEGF-A_{165}b for 30 min. **F.** Note lack of or negligible presence of tracer hot spots in these villi. **G.** Image from placenta perfused with VEGF-A_{165}a (30 min) followed by VEGF-A_{165}b (30 min) and tracer. VE-cadherin positive microvascular profiles are now a predominant feature, suggesting return of VE-cadherin to junctional regions. Concomitantly, there is minimal perivascular tracer 'hot-spots' **(H**).

Figure 5. Quantitative analyses of VE-cadherin junctional occupancy and tracer leakage in perfused placental microvascular beds.

A. Systematic counts (from 600 vascular profiles per experimental condition) revealed that in perfused placental microvascular beds VEGF-A_{165}a significantly decreased the percentage of VE-cadherin positive vascular profiles compared to VEGF-A_{165}b or vehicle only (***=P<0.001). VEGF-A_{165}b perfusion alone did not alter the % of VE-cadherin vascular profiles. In placentae where VEGF-A_{165}b was added after the 30 min VEGF-$_{165}$a perfusion, % of VE-cadherin vascular profiles were found to be similar to that of vehicle or VEGF-A_{165}b perfusions. **B.** The % of vessels showing extravasation of TRITC-dextran was significantly increased in VEGF-A_{165}a study group (**=P<0.01), but not altered when placentae were perfused with VEGF-A_{165}b when compared to vehicle only. VEGF-A_{165}b was able to reverse VEGF-A_{165}a-mediated permeability effects- the % of vascular profiles with associated peri-vascular hotspots were highly significantly reduced compared to VEGF-A_{165}a perfusions (***=P<0.001).

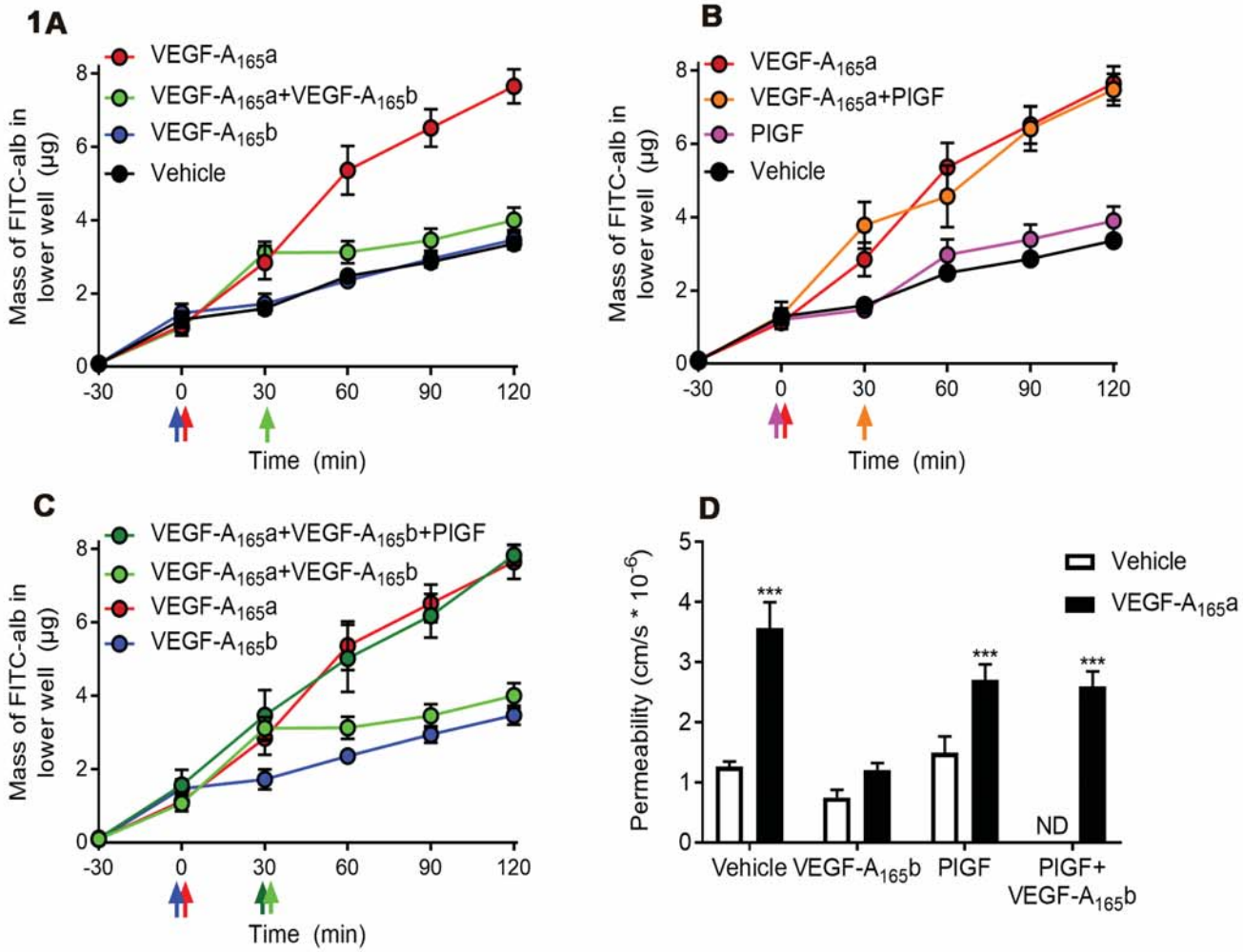
1A
VEGF-A165a
VEGF-A165a+VEGF-A165b
VEGF-A165b
Vehicle
Mass of FITC-alb in lower well (µg)
Time (min)
B
VEGF-A165a
VEGF-A165a+PIGF
PIGF
Vehicle
Mass of FITC-alb in lower well (µg)
Time (min)
C
VEGF-A165a+VEGF-A165b+PIGF
VEGF-A165a+VEGF-A165b
VEGF-A165a
VEGF-A165b
Mass of FITC-alb in lower well (µg)
Time (min)
D
Vehicle
VEGF-A165a
Permeability (cm/s * 10-6)
***
ND
Vehicle
VEGF-A165b
PIGF
PIGF+ VEGF-A165b

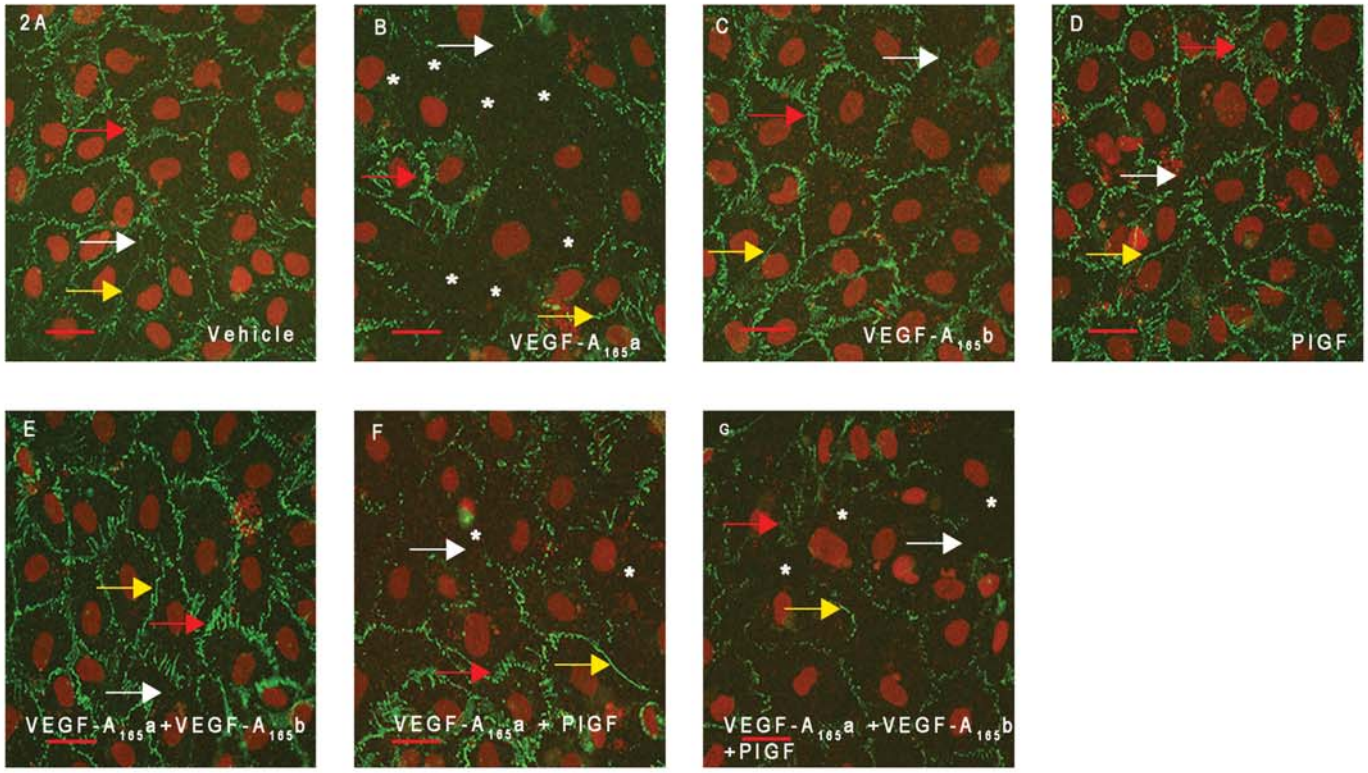
2A
Vehicle
B
VEGF-A165a
C
VEGF-A165b
D
PIGF
E
VEGF-A165a+VEGF-A165b
F
VEGF-A165a + PIGF
G
VEGF-A165a +VEGF-A165b
+PIGF

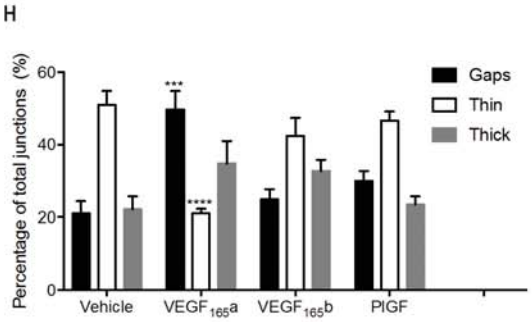
H
Percentage of total junctions (%)
60
40
20
0
***
****
Gaps
Thin
Thick
Vehicle
VEGF165a
VEGF165b
PIGF

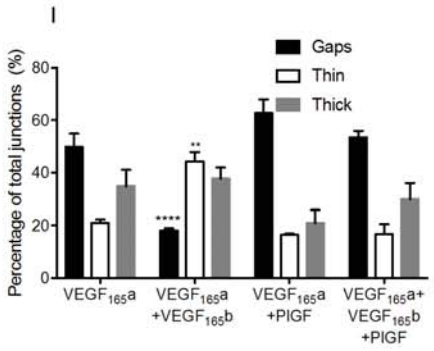
I
Percentage of total junctions (%)
80
60
40
20
0
****
**
Gaps
Thin
Thick
VEGF165a
VEGF165a
+VEGF165b
VEGF165a
+PIGF
VEGF165a+
VEGF165b
+PIGF

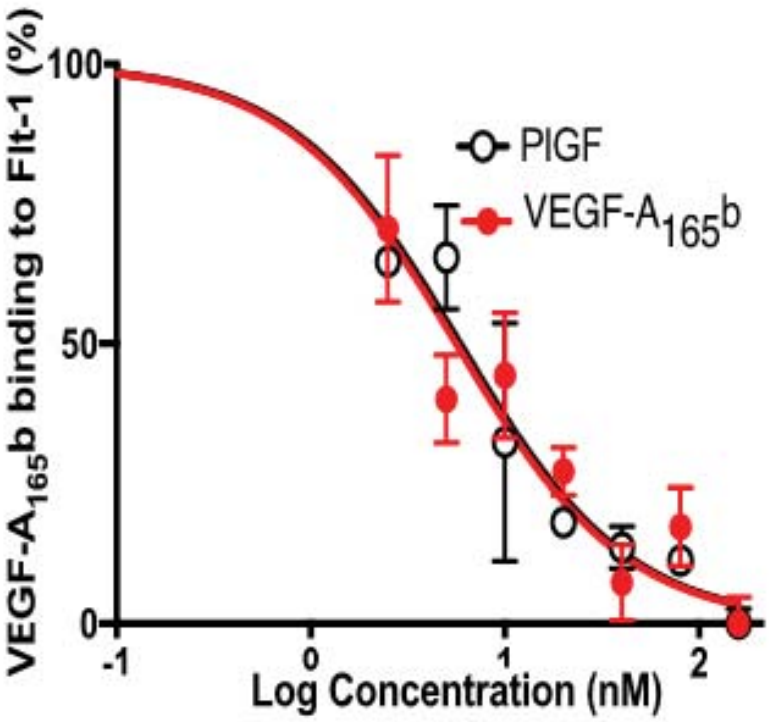

VEGF-$A_{165}b$ (IC_{50})
5.6nM (3.8-8.3)

VEGF-$A_{165}b$ (IC_{50})
5.6nM (3.8-8.3)

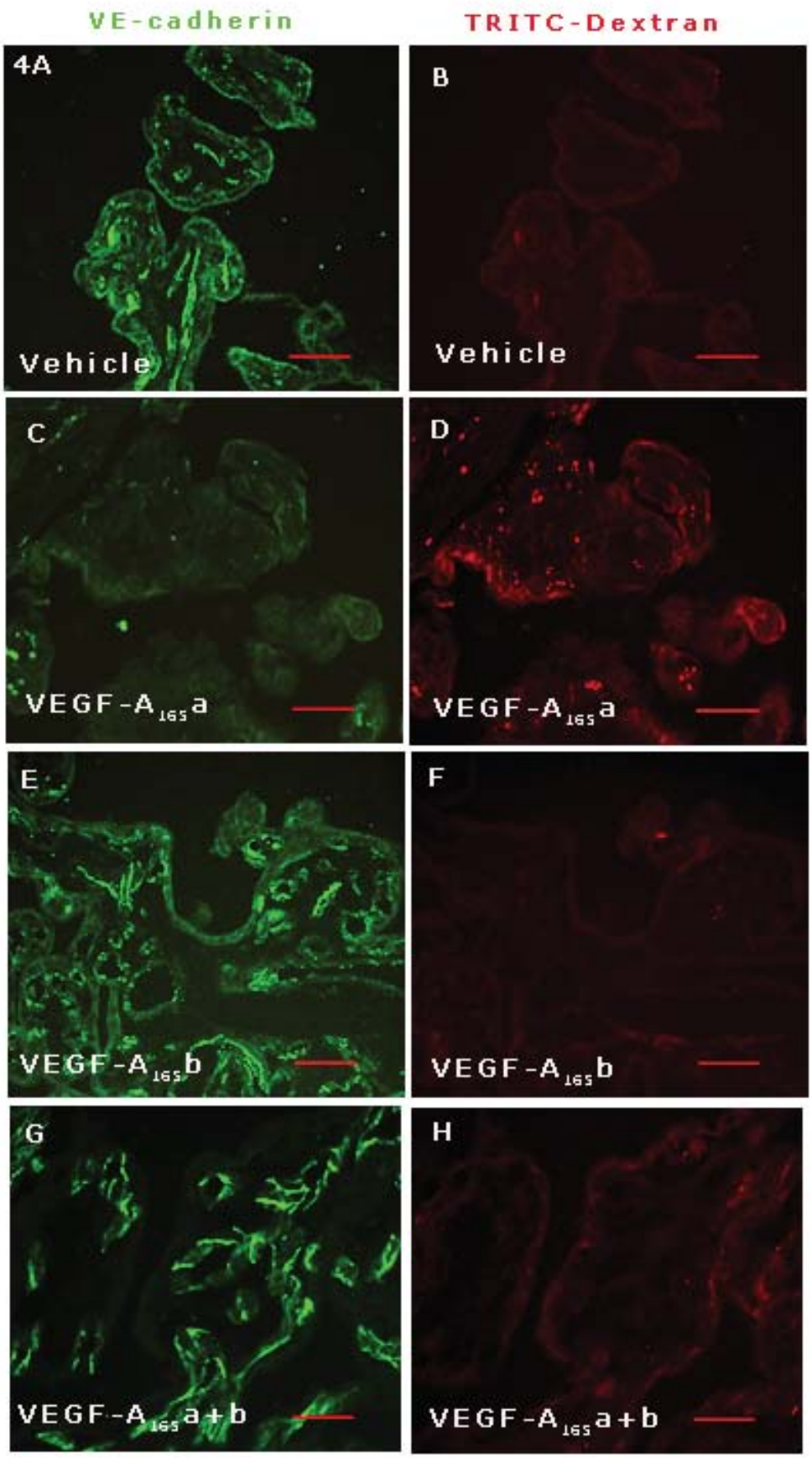
VE-cadherin
TRITC-Dextran
4A
Vehicle
B
Vehicle
C
VEGF-A165a
D
VEGF-A165a
E
VEGF-A165b
F
VEGF-A165b
G
VEGF-A165a+b
H
VEGF-A165a+b

5 A

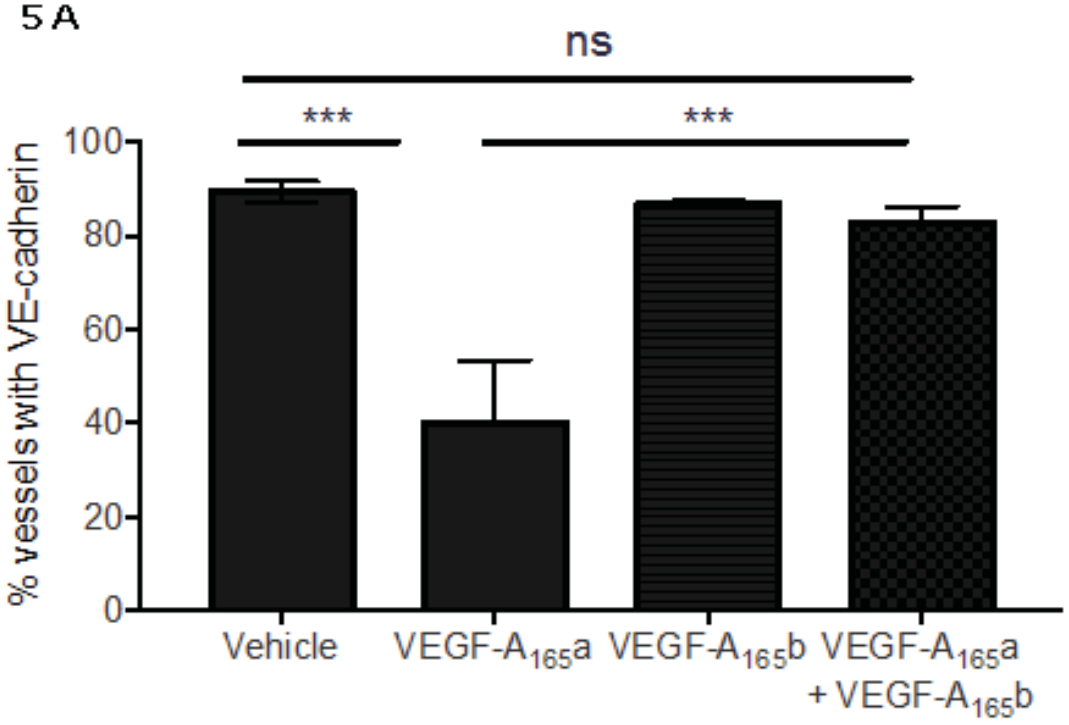
ns
***
***
% vessels with VE-cadherin
100
80
60
40
20
0
Vehicle
VEGF-A165a
VEGF-A165b
VEGF-A165a + VEGF-A165b

B

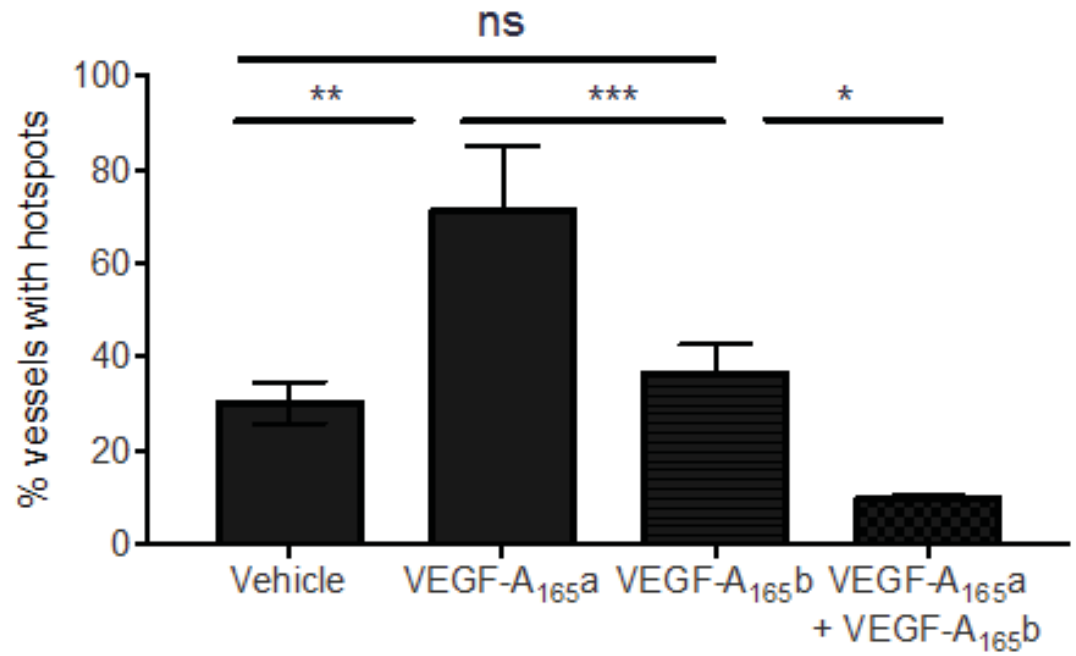
ns
**
***
*
% vessels with hotspots
100
80
60
40
20
0
Vehicle
VEGF-A165a
VEGF-A165b
VEGF-A165a + VEGF-A165b